We placed 102 seed traps at 12 levels along a 45-m high tower, with the three upper levels above the tallest trees (33 m). Traps were checked at weekly or biweekly intervals.

We surveyed all trees in a radius of 50 m around the tower. Trees were identified to species, mapped on a 2.5-m grid, and measured for DBH (diameter at breast height, 1.3 m). For a sample of at least 15 trees of each species, we measured tree height and regressed its logarithm against basal area. All regression slopes were significantly greater than zero ($P < 0.001$ in all cases) and basal area explained 61–85% of variance in tree height. We estimated height from the basal area using the regression function for trees whose heights were not measured.

We sampled the time series of the velocity components at 10 Hz using three triaxial sonic anemometers positioned at 40, 33 and 18 m above the forest floor. Plant area density (PAD) was measured with a LAI-2000 canopy analyser every 2 m, and leaf area density was inferred from PAD. A drag coefficient of 0.15 was chosen to match measured mean windspeed inside the canopy at these three levels.

Model simulations

We apply a coupled eulerian–lagrangian approach[22,23] to simulate seed dispersal from trees around the tower. We calculated statistics of wind velocities (vertical, longitudinal and lateral) inside the canopy using an eulerian second-order closure model forced by the 30-min measured friction velocity (u^*) at 40 m. Closure models, and the mixing layer analogy that describes key length and timescales of organized eddy motion for canopy flows, have been reviewed by Finnigan[29]. The lagrangian velocity used to model seed trajectories is constructed at 10 Hz in a manner that: (1) conserves coherency of intermittent eddies and (2) when averaged at a given canopy layer recovers 30-min statistics computed by the eulerian model.

We ran spatially explicit simulations of seed dispersal from all reproductive adults in a radius of 50 m around the tower. Because *P. taeda* was rare near the tower, we extended the mapping radius to 150 m for this species. Based on local observations, we define adult trees as those having DBH $\geq$ 15 cm for all species but *C. caroliniana*, for which we set a threshold of 7 cm.

The number of seeds released from each tree was linear with basal area[18]. For each simulated dispersal event, release height and seed terminal velocity were randomly selected from a normal distribution (Table 1). For each species, we estimated the vertical distribution of seed release by counting seeds or inflorescences along tree height for at least five trees. On the basis of these observations, we calculated the mean release height (Table 1) and assumed a normal distribution with a standard deviation of 0.2 of local tree height. The mean and variance of terminal velocity were estimated from video photos of falling seeds (collected at the study site), for at least 100 seeds per species. We incorporated temporal variation in wind conditions by running the model for all 1,271 half-hour averages of u^* and wind direction recorded by the upper anemometer during the simulated period.

In Fig. 2 we examine whether the bimodal patterns observed in the dispersal kernels, given spatially constant wind conditions, remain persistent when spatial variation in winds is introduced. In the first set of simulations, we assume that u^* above the canopy is constant in the plane parallel to the forest floor. Its value is related to the time-averaged shear stress above the canopy ($\tau_t = \rho u^{*2}$, where ρ is the air density), typically produced by meso-scale pressure gradients. In the second set, τ_t varies randomly in space, while keeping the same mean as in the first set (and hence the same u^*). Because the mean horizontal windspeed and vertical velocity standard deviation at any height within (or above) the canopy scale linearly with u^*, probability density functions generated from uncorrelated random normal variations of u^* in space or time converge to the ensemble average by the ergodic theorem[30]. For simplicity, the u^* variations in Fig. 2 were produced in time with a mean identical to the constant u^* scenario. However, they can be interpreted as variations of u^* in space when the number of seeds released is large (as is the case here).

Received 24 December 2001; accepted 29 April 2002; doi:10.1038/nature00844.

1. Gregory, P. H. *The Microbiology of the Atmosphere* 2nd edn (Wiley, New York, 1973).
2. Pasquill, F. & Smith, F. B. *Atmospheric Diffusion* 3rd edn (Ellis Horwood, Chichester, 1983).
3. Leonard, K. J. & Fry, W. E. (eds) *Plant Disease Epidemiology: Population Dynamics and Management* (MacMillan, New York, 1986).
4. Levin, S. A. The problem of pattern and scale in ecology. *Ecology* **73,** 1943–1967 (1992).
5. Clark, J. S. *et al.* Reid's paradox of rapid plant migration: dispersal theory and interpretation of paleoecological records. *Bioscience* **48,** 13–24 (1998).
6. Cain, M. L., Milligan, B. G. & Strand, A. E. Long-distance seed dispersal in plant populations. *Am. J. Bot.* **87,** 1217–1227 (2000).
7. Nathan, R. & Muller-Landau, H. C. Spatial patterns of seed dispersal, their determinants and consequences for recruitment. *Trends Ecol. Evol.* **15,** 278–285 (2000).
8. Nathan, R. in *Encyclopedia of Biodiversity* Vol. II (ed. Levin, *S. A.) 127–152 (Academic Press, San Diego, 2001).*
9. Greene, D. F. & Johnson, E. A. Long-distance wind dispersal of tree seeds. *Can. J. Bot.* **73,** 1036–1045 (1995).
10. Higgins, S. I. & Richardson, D. M. Predicting plant migration rates in a changing world: the role of long-distance dispersal. *Am. Nat.* **153,** 464–475 (1999).
11. Bullock, J. M. & Clarke, R. T. Long distance seed dispersal by wind: measuring and modelling the tail of the curve. *Oecologia* **124,** 506–521 (2000).
12. Clark, J. S., Lewis, M. & Horvath, L. Invasion by extremes: population spread with variation in dispersal and reproduction. *Am. Nat.* **157,** 537–554 (2001).
13. Ridley, H. N. *The Dispersal of Plants Throughout the World* (Reeve, Ashford, 1930).
14. van der Pijl, L. *Principles of Dispersal in Higher Plants* 3rd edn (Springer, Berlin, 1982).
15. Ridley, H. N. On the dispersal of seeds by wind. *Ann. Bot. Lond.* **19,** 351–363 (1905).
16. Webber, M. L. Fruit dispersal. *Malayan Forester* **3,** 18–19 (1934).
17. Willson, M. F. Dispersal mode, seed shadows, and colonization patterns. *Vegetatio* **107/108,** 261–280 (1993).
18. Clark, J. S., Macklin, E. & Wood, L. Stages and spatial scales of recruitment limitation in southern Appalachian forests. *Ecol. Monogr.* **68,** 213–235 (1998).
19. Okubo, A. & Levin, S. A. A theoretical framework for data analysis of wind dispersal of seeds and pollen. *Ecology* **70,** 329–338 (1989).
20. Nathan, R., Safriel, U. N. & Noy-Meir, I. Field validation and sensitivity analysis of a mechanistic model for tree seed dispersal by wind. *Ecology* **82,** 374–388 (2001).
21. Hsieh, C. I., Katul, G. G., Schieldge, J., Sigmon, J. T. & Knoerr, K. K. The Lagrangian stochastic model for fetch and latent heat flux estimation above uniform and nonuniform terrain. *Water Resour. Res.* **33,** 427–438 (1997).
22. Katul, G. G. & Albertson, J. D. An investigation of higher-order closure models for a forested canopy. *Boundary-Lay. Meteorol.* **89,** 47–74 (1998).
23. Higgins, S. I., Nathan, R. & Cain, M. L. Are long-distance dispersal events in plants usually caused by nonstandard means of dispersal? *Ecology* (submitted).
24. Katul, G. G., Geron, C. D., Hsieh, C. I., Vidakovic, B. & Guenther, A. B. Active turbulence and scalar transport near the forest–atmosphere interface. *J. Appl. Meteor.* **37,** 1533–1546 (1998).
25. Burns, R. M. & Honkala, B. H. *Silvics of North America. Agricultural Handbook 654* (US Department of Agriculture, Washington, DC, 1990).
26. De Steven, D. Experiments on mechanisms of free establishment in old-field succession: seedling survival and growth. *Ecology* **72,** 1076–1088 (1991).
27. Nathan, R. The challenges of studying dispersal. *Trends Ecol. Evol.* **16,** 481–483 (2001).
28. Horn, H. S., Nathan, R. & Kaplan, S. R. Long-distance dispersal of tree seeds by wind. *Ecol. Res.* **16,** 877–885 (2001).
29. Finnigan, J. Turbulence in plant canopies. *Ann. Rev. Fluid Mech.* **32,** 519–571 (2000).
30. Monin, A. S. & Yaglom, A. M. in *Statistical Fluid Mechanics* Vol. 1 (ed. Lumley, J.) 209–218 (MIT Press, Cambridge, Massachusetts, 1971).

Acknowledgements

We thank M. Siqueira, C.-T. Lai, C.-I. Hsieh, I. Ibanez, S. LaDeau, B. Poulter, D. Ellsworth, J. Chave and O. Nathan for their help with data collection, and M. Cain for his comments. This study is supported by the National Science Foundation and the US Department of Energy through their Integrative Biology and Neuroscience, Terrestrial Carbon Processes, and National Institute for Global Environmental Change (South-East Regional Center) programmes.

Competing interests statement

The authors declare that they have no competing financial interests.

Correspondence and requests for materials should be addressed to R.N. (e-mail: rnathan@bgumail.bgu.ac.il).

A neural correlate of response bias in monkey caudate nucleus

Johan Lauwereyns*, Katsumi Watanabe*, Brian Coe† & Okihide Hikosaka*

** Laboratory of Sensorimotor Research, National Eye Institute, Building 49, Room 2A50, National Institutes of Health, Bethesda, Maryland 20892, USA*
† Department of Physiology, Juntendo University, 2-1-1 Hongo, Bunkyo-ku, Tokyo 113-0033, Japan

Primates are equipped with neural circuits in the prefrontal cortex[1–6], the parietal cortex[7] and the basal ganglia[6,8–11] that predict the availability of reward during the performance of behavioural tasks. It is not known, however, how reward value is incorporated in the control of action. Here we identify neurons in the monkey caudate nucleus that create a spatially selective response bias depending on the expected gain. In behavioural tasks, the monkey had to make a visually guided eye movement in every trial, but was rewarded for a correct response in only half of the trials. Reward availability was predictable on the basis of the spatial position of the visual target. We found that caudate neurons change their discharge rate systematically, even before the appearance of the visual target, and usually fire more when the contralateral position is associated with reward. Strong anticipatory activity of neurons with a contralateral preference is associated with decreased latency for eye movements in the contralateral direction. We conclude that this neuronal mechan-

ism creates an advance bias that favours a spatial response when it is associated with a high reward value.

Reward shapes goal-oriented behaviour[12–14]. Consider a visually guided saccade task with an asymmetrical reward schedule (Fig. 1a and b, biased saccade task; BST). The monkey has to make an immediate saccade to a peripheral visual target in every trial, but is rewarded for a correct saccade to only one out of two possible target positions. The mapping between target position and reward remains constant for 20 or 40 trials, but is reversed frequently during an experimental session (Fig. 1c and Methods).

In this task, the average latency of saccadic eye movements was reliably shorter in trials with reward than in trials without reward. Figure 1d shows the rightward saccades of monkey 1; saccade latency was 88 ms shorter in reward than in no-reward trials ($P < 0.01$, two-tailed t-test). The reward effect amounted to 53 ms for the leftward saccades of monkey 1, 141 ms for the rightward saccades of monkey 2, and 203 ms for the leftward saccades of monkey 2; all three effects were significant ($P < 0.01$, two-tailed t-test). Although previous research has identified neural circuits that encode the presence of reward[1–11], little is known about how such representations may cause the reward effect in the behaviour. Here we explored the possibility that the brain creates a reward-oriented response bias before the presentation of an instruction on where to move the eyes.

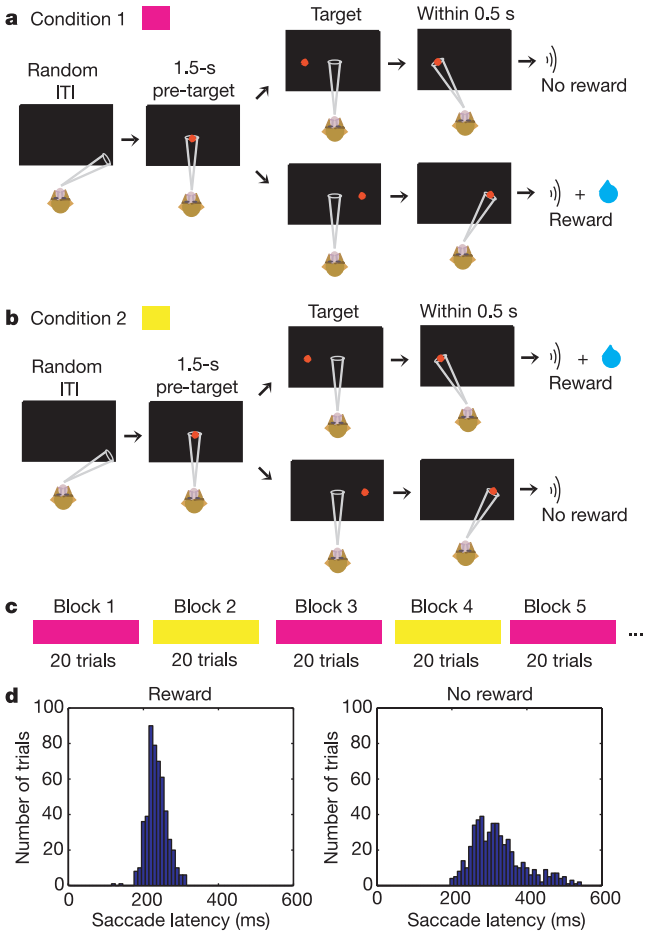

Figure 1 Experimental design of the biased saccade task (BST). **a**, Sequence of events in condition 1, in which only correct rightward saccades are rewarded. **b**, Sequence of events in condition 2, in which only correct leftward saccades are rewarded. **c**, Blocked ('ABA') design with frequent repetitions of different conditions. **d**, Density function of saccade latency in reward trials versus no-reward trials (data from monkey 1, rightward saccades).

We concentrated on caudate neurons that selectively increased their discharge rate right before the expected appearance of a task-relevant visual target[8,15–16]. On the basis of their discharge characteristics[17], we assumed that these neurons were medium-spiny[18], GABA (γ-amino butyric acid)-mediated[19] projection neurons. Using a memory-guided saccade task[20], we previously found that

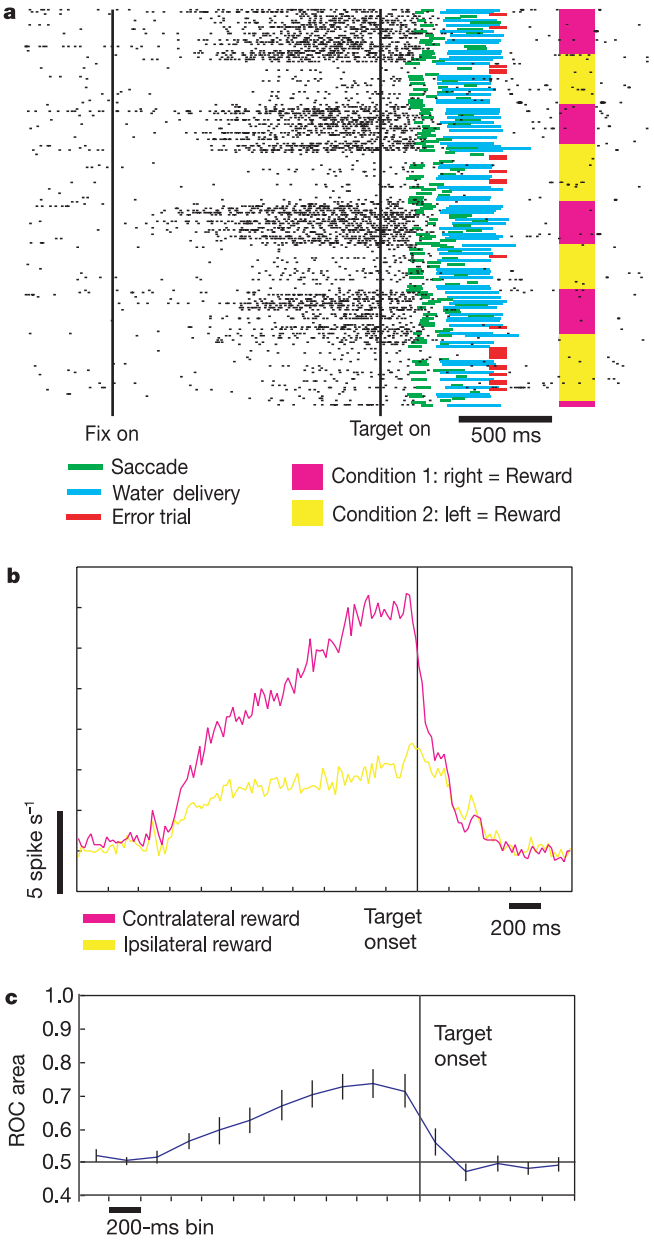

Figure 2 Effect of position-reward mapping on caudate anticipatory activity. **a**, Rasters of spikes aligned with target onset. Each raster represents one trial; trials are shown in order of presentation (from top to bottom). Green bars indicate saccade duration, blue bars indicate water delivery, red bars indicate error trial. Colour codes to the right of the rasters indicate the position-reward condition (yellow, left reward; purple, right reward). **b**, Population histograms of the activity of caudate neurons with a contralateral pre-target bias ($n = 25$). The histograms are aligned with target onset (yellow, ipsilateral reward; purple, contralateral reward). **c**, Area under the receiver operating characteristic (ROC area) in a sliding 200-ms window. Shown here is the average ROC area (±95% confidence interval) from the same population of neurons as in **b**. The ROC area quantifies the separation of the distributions in the contralateral and ipsilateral reward conditions (0.5, no separation; 1, perfect contralateral preference; 0, perfect ipsilateral preference).

the anticipatory activity of these neurons is sensitive to the contingency between stimulus and reward[21–22]. In the memory-guided saccade task, however, the delay between target presentation and saccade prevented us from studying the relationship between neuronal activity and behavioural parameters. Thus, to test whether caudate neurons create an advance response bias, we examined their activity in the BST, in which the monkey had to make an immediate visually guided saccade under an asymmetrical reward schedule. Forty-one caudate neurons with anticipatory activity provided sufficient data for analysis. Of these 41 neurons, 31 (76%) showed a reliable effect of position-reward mapping in their anticipatory activity ($P < 0.01$ in the window of -1.5 s to 0 s from target onset, two-tailed t-test), and usually fired more when the contralateral position was mapped onto reward than when the ipsilateral position was mapped onto reward (25/31; 81%). The remaining six neurons, with a preference for the ipsilateral-reward condition, behaved in all respects as the mirror image of neurons with a preference for the contralateral-reward condition.

The pre-target component in the caudate neurons showed marked selectivity. For the neuron shown in Fig. 2a, for example, the session started with a right (or contralateral) reward block, followed by an ipsilateral-reward block, then a contralateral-reward block again, and so on. Clearly, the neuron fired consistently more strongly in the contralateral-reward condition than in the ipsilateral-reward condition. This highly adaptive pre-target component cannot be explained by arousal, fixation-related activity or any other interpretation that does not take into account the context of the position-reward mapping. In Fig. 2b and c, we present population data of 25 caudate neurons that showed a similar preference for the contralateral-reward condition in their pre-target activity. The modulation by reward context started more than 1 s before target onset and reached a plateau by about 400 ms before target onset. The effect quickly dissipated after target onset. This time course clearly suggests that the pre-target component is prospective, in anticipation of the eye movement instruction.

For each of the 31 neurons with a reliable pre-target bias, we also obtained a reliable reward effect in the monkey's behaviour ($P < 0.01$, two-tailed t-test). This result confirmed that modulation of the pre-target component occurred together with the reward-dependent effects in saccade latency. Could the pre-target com-

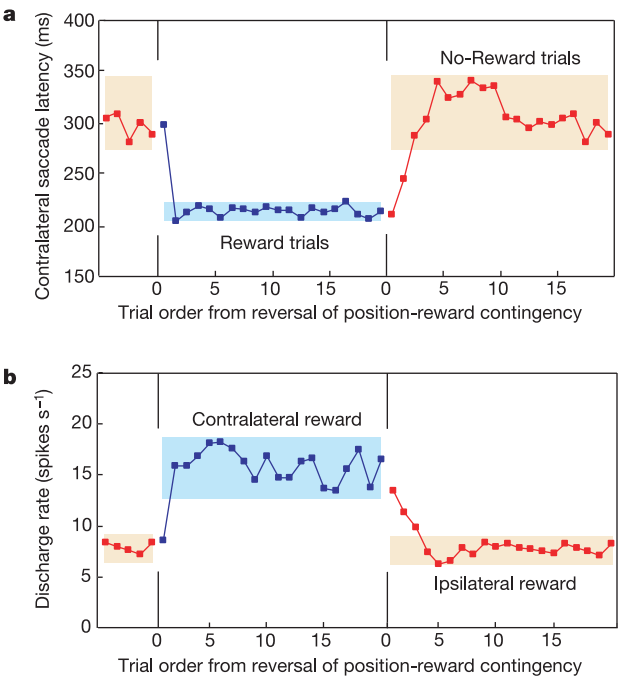

Figure 3 Adaptation of behaviour and neuronal activity to a reversal of the position-reward contingency. **a**, Latency for contralateral saccades as a function of trial order from reversal of position-reward contingency. Blue data indicate reward trials; red data indicate no-reward trials. Coloured backgrounds indicate the areas ± 2 s.d. from the mean in trials 6–20 (light blue, reward trials; light orange, no-reward trials). **b**, Neuronal discharge rate as a function of trial order from reversal of position-reward contingency. Shown are data from neurons with a contralateral pre-target bias (the same population of neurons as in Fig. 2b,c; same data set as in **a**). Blue data, trials in the contralateral-reward condition; red data, trials in the ipsilateral-reward condition. Coloured backgrounds indicate the areas ± 2 s.d. from the mean in trials 6–20 (light blue, contralateral-reward condition; light orange, ipsilateral-reward condition).

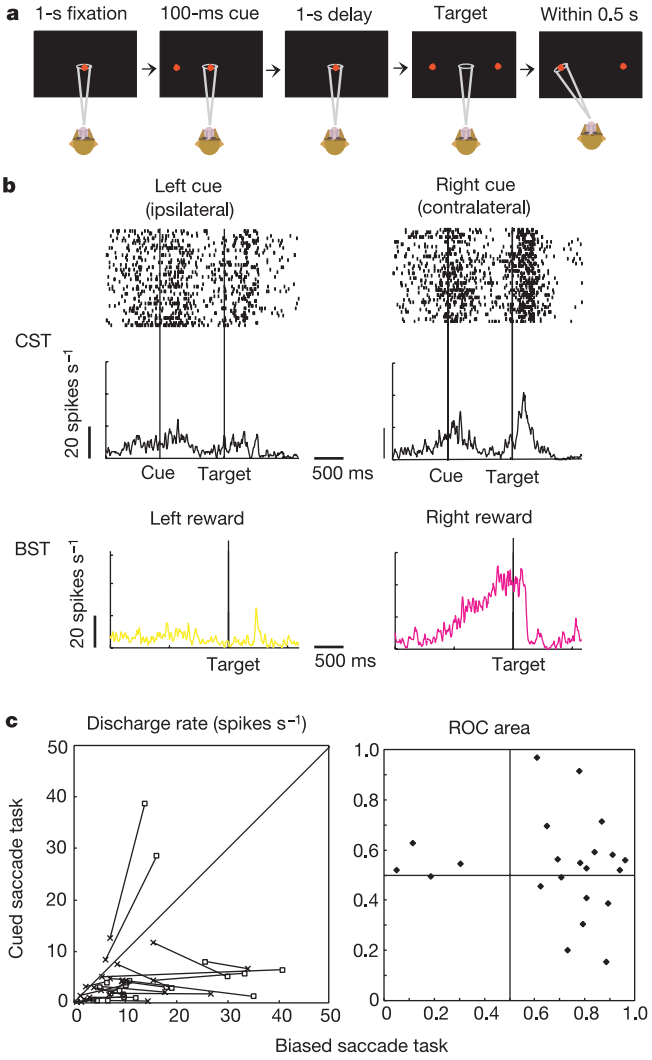

Figure 4 Comparison between the cued saccade task (CST) and the biased saccade task (BST). **a**, Sequence of events in CST. **b**, Top, rasters and histograms from a caudate neuron grouped by the spatial position of the cue in CST (top). Bottom, histograms for BST are shown for comparison (purple, left-reward condition; yellow, right-reward condition). **c**, Scatter plots of neuronal activity in CST versus BST. Data from 22 caudate neurons with a spatial pre-target bias in BST are shown. On the left, a line is drawn between two data points for each neuron: the data point indicated by a cross represents activity in the ipsilateral condition (vertical coordinate, ipsilateral cue in CST; horizontal coordinate, ipsilateral reward in BST); the data point indicated by a square represents activity in the contralateral condition in CST versus BST. On the right, each data point indicates the ROC areas of one neuron in the two tasks. ROC areas quantify the separation between ipsilateral and contralateral distributions (0.5, no separation; 1, perfect contralateral preference; 0, perfect ipsilateral preference). Vertical coordinate, ROC area in CST; horizontal coordinate, ROC area in BST.

ponent be a source of the reward effect in saccade latency? One interpretation is that the pre-target component acts as a spatial response bias, which prioritizes an eye movement toward the neuron's preferred position if that position is associated with a high reward value. Specifically, a strong pre-target component when the contralateral position is associated with reward will favour an eye movement to the contralateral position. When this position is no longer associated with reward, the weak pre-target component will lead to a reduced priority of an eye movement to the contralateral position.

The interpretation of caudate pre-target activity as a spatial response bias finds support in the way in which the monkey's behaviour and neuronal activity adapted to changes in the reward context (Fig. 3). We compared the latency for contralateral saccades with the pre-target activity (from −1.5 s to 0 s from target onset) of neurons with a preference for the contralateral-reward condition. Even though the monkey made saccades in each direction equally often (see Methods), we focused only on contralateral saccades for this analysis because we thought that there might be an association between contralateral saccades and the activity of neurons with a contralateral preference. Specifically, we examined how many trials it took for the contralateral-saccade latency and the selectivity in the neuronal activity to adapt to a reversal of the contingency between position and reward. In the latency for contralateral saccades (Fig. 3a), there was a notable asymmetry such that the reduction of latency in reward trials (the positive effect of incentive) was fully present from the second trial after a reversal, that is, immediately after the monkey experienced a change in reinforcement. The increase of latency in no-reward trials (the negative effect of no incentive) developed more slowly, reaching a peak at the fifth trial.

In the neuronal pre-target activity (Fig. 3b), we observed a similar asymmetry in the adaptation to a reversal. The increase of pre-target activity in the contralateral-reward condition was in full effect from the second trial after a reversal. This finding is consistent with the quick adaptation of the positive effect of incentive, assuming that strong pre-target activity leads to short latency for contralateral saccades. In contrast, the decrease of pre-target activity in the ipsilateral-reward condition developed more slowly, reaching a peak at the fifth trial. Again, this finding is consistent with the slow adaptation of the negative effect of no incentive, assuming that weak pre-target activity leads to long latency for contralateral saccades.

The slow versus fast adaptation after a reversal in the caudate pre-target activity might be related to different learning rates for positive-reward contingency (a contingency between the contralateral position and reward) than for negative-reward contingency (a contingency between the contralateral position and no reward)[23]. Such asymmetry would in turn influence the development of the reward effect in the monkey's behaviour. Although the underlying mechanisms are not fully understood, the implication here is that there is tight coupling between the spatial pre-target bias in caudate neuronal activity and the reward effect in behaviour.

Although the pre-target component in caudate neurons seems to incorporate reward value in advance of the process of action control, it is possible that it represents an instance of a more general type of spatially selective anticipation. Specifically, previous research has documented spatially selective effects of target uncertainty on the anticipatory activity of neurons in parietal cortex[7] and superior colliculus[24,25]. Are effects of reward context and target uncertainty caused by similar neural mechanisms of anticipation? To test this possibility, we examined 22 of the 31 caudate neurons with a spatial pre-target bias in a second experiment, the cued saccade task (CST; Fig. 4). In this task, the monkey was required to make a saccade to a target that appeared at a previously cued position. The probability that a target appeared at the cued position was 100%. In half of the trials, we presented a distracter in addition to the target, so that the monkey needed to process the cue position to distinguish target from distracter. Thus, correct task performance depended on the monkey's ability to select a spatial position on the basis of information provided in advance of target onset. Both monkeys performed this task with an error rate of less than 10% even in trials with a distracter, which indicates that they do rely on the spatial position of the cue.

Whereas the example neuron in Fig. 4b showed no effect of cue position in its activity in the window from −500 ms to 0 ms before target onset in the CST (Fig. 4b, top), it showed a clear contralateral pre-target bias in the same time window before target onset in the BST (Fig. 4b, bottom). For all but two neurons the laterality effect was stronger in the BST than in the CST (that is, longer extension in the horizontal than in the vertical axis; Fig. 4c, left), and there was no correlation between laterality effects in the different tasks (the Pearson correlation coefficient of the receiver operating characteristic (ROC) areas is −0.125, which is not significantly different from zero; Fig. 4c, right). These results suggest that the caudate pre-target component is influenced by reward context, but not by target uncertainty. Further research is required to determine whether the caudate pre-target component can be influenced by other factors than reward.

In summary, the context of stimulus-reward mapping strongly modulates both the pre-target activity in caudate neurons and the latency of saccadic eye movements. The pre-target bias in caudate nucleus may be one of the ways in which the brain incorporates reward value in the control of action, even before the presentation of a visual instruction on where to move the eyes. By this interpretation, the bias in caudate nucleus favours a particular spatial response when it is associated with a high reward value, but not when it is associated with a low reward value. Such a response bias in the caudate nucleus could be propagated through a sequence of two inhibitory projections, from caudate nucleus onto substantia nigra pars reticulata, and then onto superior colliculus[26–28]. Specifically, the caudate pre-target bias might lead to a spatially selective removal of tonic inhibition from substantia nigra pars reticulata on superior colliculus neurons with a particular movement field. The effect from caudate nucleus on superior colliculus would be to pre-establish a different baseline of neuronal activity in the contralateral-reward versus ipsilateral-reward condition. Thus, the caudate bias would bring superior colliculus neurons with a movement field to the position with a high reward value closer to initiating a saccade, even before the presentation of a visual instruction. □

Methods

Electrophysiological recording

We recorded from the caudate nuclei of two adult male Japanese monkeys (*Macaca fuscata*). Surgery was carried out under pentobarbital sodium anaesthesia to implant a head-holding device, a plastic unit-recording chamber and a scleral search coil. The recording chamber was placed over the fronto-parietal cortices, tilted laterally by 35° in the coronal plane, and aimed at the caudate head, as verified by magnetic resonance imaging (AIRIS, 0.3 T, Hitachi). Action potentials of single neurons were recorded with tungsten electrodes, which were advanced perpendicularly to the cortical surface using an oil-driven micro-manipulator (MO-95, Narishige). The action potentials were amplified, filtered (500 to 2,000 Hz) and processed by a window discriminator (MDA-4 and DDIS-1, BAK Electronics). We recorded eye movements using the magnetic search-coil technique (MEL-25, Enzanshi-Kogyo). All surgical and experimental protocols were approved by the Juntendo University Animal Care and Use Committee, and were in accordance with the NIH Guidelines for Care and Use of Animals.

Behavioural task

The monkey sat in a primate chair inside a sound-attenuated room with his head fixed. In the BST, the monkey was required to direct and maintain his gaze at a central fixation spot during a first fixation ('pre-target') period of 1.5 s. Visual stimuli were small red spots, 0.2° in diameter, back-projected onto a tangent screen by LED projectors. After the pre-target period, the fixation spot disappeared and a peripheral target appeared at 20° to the left or to the right. The monkey had to make a saccade within 500 ms to within 3° from the target position. A beep was presented as feedback for each correct trial. If the monkey made an error, the same trial was repeated. In half of the correct trials the monkey was rewarded with a drop of water depending on the reward schedule. During blocks of 20 or 40 correct trials, reward was mapped consistently onto one target position. We reversed the position-

reward contingency automatically (6–16 times) without any indication to the monkey.

There were various types of error trial: failing to fixate the fixation point, breaking fixation before fixation offset, making a saccade in the wrong direction, and making a hypo- or hypermetric saccade in the right direction. Because it can be difficult to relate caudate pre-target activity to the various types of error trial, we limited our focus in the present paper to correct trials. Our behavioural procedure ensured that we had an equal amount of data from correct trials in the reward condition and those in the no-reward condition.

In the CST, there was a first fixation period of 1 s, followed by a brief presentation (100 ms) of a cue at 20° to the left or to the right. The monkey had to maintain his gaze at the fixation spot during a delay period of 1 s. The fixation spot then disappeared and the target appeared at the same position as the cue. In half of the trials, another spot appeared at the alternative position (distracter). The monkey had to make a saccade to the target position within 500 ms, and was rewarded with a drop of water for a correct saccade. After recording neurons in the CST (experiment 2), we re-applied the BST (experiment 1) for at least 80 trials to confirm the reproducibility of neuronal activity.

Data analysis

Pre-target neurons were defined as neurons that showed a statistically reliable increase in the spike count −1.5 s to 0 s before target onset ('pre-target window') as compared with the spike count −3 s to −1.5 s before target onset. All pair-wise comparisons were evaluated by two-tailed *t*-tests, $P < 0.01$. We used the Bonferroni procedure to correct for family-wise error with multiple *t*-tests. To quantify the separation of population distributions from contralateral versus ipsilateral conditions, we calculated the area under the ROC in a sliding window of 200 ms.

To test the adaptation of saccade latency and pre-target activity to a reversal of position-reward contingency, we compared the second trial after a reversal against the third trial after a reversal (test 1). We also compared the second trial after a reversal against the pooled data from the sixth to twentieth trial (test 2). Both tests consisted of paired two-tailed *t*-tests on the mean data from individual neurons. Adaptation was judged complete if there was no significant difference between the measures. Tests 1 and 2 produced similar results in all cases.

For comparison between the two tasks (BST versus CST), we considered the neuronal activity from −500 to 0 ms before target onset in both tasks, in the computation of absolute firing rates as well as ROC areas.

Received 25 January; accepted 20 May 2002; doi:10.1038/nature00892.

1. Amador, N., Schlag-Rey, M. & Schlag, J. Reward-predicting and reward-detecting neuronal activity in the supplementary eye field. *J. Neurophysiol.* **84,** 2166–2170 (2000).
2. Kobayashi, S., Lauwereyns, J., Koizumi, M., Sakagami, M. & Hikosaka, O. Influence of reward expectation on visuospatial processing in macaque lateral prefrontal cortex. *J. Neurophysiol.* **87,** 1488–1498 (2002).
3. Leon, M. I. & Shadlen, M. N. Effect of expected reward magnitude on the response of neurons in the dorsolateral prefrontal cortex of the macaque. *Neuron* **24,** 415–425 (1999).
4. Tremblay, L. & Schultz, W. Relative reward preference in primate orbitofrontal cortex. *Nature* **398,** 704–708 (1999).
5. Watanabe, M. Reward expectancy in primate prefrontal neurons. *Nature* **382,** 629–632 (1996).
6. Rolls, E. T. *The Brain and Emotion* (Oxford Univ. Press, New York, 1999).
7. Platt, M. L. & Glimcher, P. W. Neural correlates of decision variables in parietal cortex. *Nature* **400,** 233–238 (1999).
8. Hikosaka, O., Sakamato, M. & Usui, S. Functional properties of monkey caudate neurons. III. Activities related to expectation of target and reward. *J. Neurophysiol.* **61,** 814–832 (1989).
9. Kawagoe, R., Takikawa, Y. & Hikosaka, O. Expectation of reward modulates cognitive signals in the basal ganglia. *Nature Neurosci.* **1,** 411–416 (1998).
10. Schultz, W., Apicella, P., Scarnati, E. & Ljungberg, T. Neuronal activity in monkey ventral striatum related to the expectation of reward. *J. Neurosci.* **12,** 4595–4610 (1992).
11. Schultz, W., Dayan, P. & Montague, P. R. A neural substrate of prediction and reward. *Science* **275,** 1593–1599 (1997).
12. Bindra, D. Neuropsychological interpretation of the effects of drive and incentive-motivation on general activity and instrumental behaviour. *Psychol. Rev.* **75,** 1–22 (1968).
13. Dickinson, A. & Baleine, B. Motivational control of goal-directed action. *Anim. Learn. Behav.* **22,** 1–18 (1994).
14. Watanabe, M. *et al.* Behavioral reactions reflecting differential reward expectations in monkeys. *Exp. Brain Res.* **140,** 511–518 (2001).
15. Apicella, P., Scarnati, E., Ljungberg, T. & Schultz, W. Neuronal activity in monkey striatum related to the expectation of predictable environmental events. *J. Neurophysiol.* **68,** 945–960 (1992).
16. Rolls, E. T., Thorpe, S. J. & Maddison, S. P. Responses of striatal neurons in the behaving monkey. I. Head of the caudate nucleus. *Behav. Brain Res.* **7,** 179–210 (1983).
17. Hikosaka, O., Sakamato, M. & Usui, S. Functional properties of monkey caudate neurons. I. Activities related to saccadic eye movements. *J. Neurophysiol.* **61,** 780–798 (1989).
18. Kawaguchi, Y., Wilson, C. J. & Emson, P. C. Projection subtypes of rat neostriatal matrix cells revealed by intracellular injection of biocytin. *J. Neurosci.* **10,** 3421–3438 (1990).
19. Fisher, R. S., Buchwald, N. A., Hull, C. D. & Levine, M. S. The GABAergic striatonigral neurons of the cat: Demonstration by double peroxidase labeling. *Brain Res.* **398,** 148–156 (1986).
20. Hikosaka, O. & Wurtz, R. H. Visual and oculomotor functions of monkey substantia nigra pars reticulata. III. Memory-contingent visual and saccade responses. *J. Neurophysiol.* **49,** 1268–1284 (1983).
21. Lauwereyns, J. *et al.* Feature-based anticipation of cues that predict reward in monkey caudate nucleus. *Neuron* **33,** 463–473 (2002).
22. Takikawa, Y., Kawagoe, R. & Hikosaka, O. Reward-dependent spatial selectivity of anticipatory activity in monkey caudate neurons. *J. Neurophysiol.* **87,** 508–515 (2002).
23. Rescorla, R. A. & Wagner, A. R. in *Classical Conditioning II: Current Research and Theory* (eds Black, A. H. & Prokasy, W. F.) 64–99 (Appleton Century Crofts, New York, 1972).
24. Basso, M. A. & Wurtz, R. H. Modulation of neuronal activity by target uncertainty. *Nature* **389,** 66–69 (1997).
25. Dorris, M. C. & Munoz, D. P. Saccadic probability influences motor preparation signals and time to saccadic initiation. *J. Neurosci.* **18,** 7015–7026 (1998).
26. Hikosaka, O., Kawagoe, R. & Takikawa, Y. Role of the basal ganglia in the control of purposive saccadic eye movements. *Physiol. Rev.* **80,** 953–978 (2000).
27. Ikeda, T., Takikawa, Y. & Hikosaka, O. Visuo-motor and anticipatory activities of monkey superior colliculus neurons are modulated by reward. *Soc. Neurosci. Abstr.* **27,** 59.1 (2001).
28. Sato, M. & Hikosaka, O. Role of primate substantia nigra pars reticulata in reward-oriented saccadic eye movement. *J. Neurosci.* **22,** 2363–2373 (2002).

Acknowledgements

We thank H. Nakahara, Y. Shimo, M. Sato, Y. Takikawa, R. Kawagoe, H. Itoh, S. Kobayashi, M. Koizumi and M. Sakagami for comments and technical assistance. This research was supported by the Japanese Society for the Promotion of Science.

Competing interests statement

The authors declare that they have no competing financial interests.

Correspondence and requests for materials should be addressed to O.H. (e-mail: oh@lsr.nei.nih.gov).

Post-translational disruption of dystroglycan–ligand interactions in congenital muscular dystrophies

Daniel E. Michele*, Rita Barresi*, Motoi Kanagawa*, Fumiaki Saito*, Ronald D. Cohn*, Jakob S. Satz*, James Dollar†, Ichizo Nishino‡, Richard I. Kelley§, Hannu Somer‖, Volker Straub*, Katherine D. Mathews¶, Steven A. Moore# & Kevin P. Campbell*

* *Howard Hughes Medical Institute, Department of Physiology and Biophysics, and Department of Neurology;* ¶ *Department of Pediatrics; and* # *Department of Pathology, University of Iowa, Iowa City, Iowa 52242-1101, USA*
† *Department of Pathology, Albany Medical College, Albany, New York 12208, USA*
‡ *Department of Neuromuscular Research, National Institute of Neuroscience, Tokyo 187-8502, Japan*
§ *Kennedy Krieger Institute, John Hopkins University, Baltimore, Maryland 21205, USA*
‖ *Department of Neurology, Helsinki University Hospital, 00029 HUS Helsinki, Finland*

Muscle–eye–brain disease (MEB) and Fukuyama congenital muscular dystrophy (FCMD) are congenital muscular dystrophies with associated, similar brain malformations[1,2]. The FCMD gene, *fukutin*, shares some homology with *fringe*-like glycosyltransferases, and the MEB gene, *POMGnT1*, seems to be a new glycosyltransferase[3,4]. Here we show, in both MEB and FCMD patients, that α-dystroglycan is expressed at the muscle membrane, but similar hypoglycosylation in the diseases directly abolishes binding activity of dystroglycan for the ligands laminin, neurexin and agrin. We show that this post-translational biochemical and functional disruption of α-dystroglycan is recapitulated in the muscle and central nervous system of mutant myodystrophy (*myd*) mice. We demonstrate that *myd* mice have abnormal neuronal migration in cerebral cortex, cerebellum and hippocampus, and show disruption of the basal lamina. In addition, *myd* mice reveal that dystroglycan targets proteins to functional sites in brain through its interactions with extracellular matrix proteins. These results suggest that at least three distinct mammalian genes function within a convergent post-translational processing pathway during the biosynthesis of dystroglycan, and that abnormal dystroglycan–ligand interactions underlie the pathogenic mechanism of muscular dystrophy with brain abnormalities.